 CMC, vol.53, no.3, pp.249-270, 2017

Mathematical Modelling and 3D FEM Analysis of the Influence of Initial Stresses on the ERR in a Band Crack's Front in the Rectangular Orthotropic Thick Plate

Arzu Turan Dincel[1] and Surkay D. Akbarov [2,3]

Abstract: This paper deals with the mathematical modelling and 3D FEM study of the energy release rate (ERR) in the band crack's front contained in the orthotropic thick rectangular plate which is stretched or compressed initially before the loading of the crack's edge planes. The initial stretching or compressing of the plate causes uniformly distributed normal stress to appear acting in the direction which is parallel to the plane on which the band crack is located. After the appearance of the initial stress in the plate it is assumed that the crack's edge planes are loaded with additional uniformly distributed normal forces and the ERR caused with this additional loading is studied. The corresponding boundary value problem is formulated within the scope of the so-called 3D linearized theory of elasticity which allows the initial stress on the values of the ERR to be taken into consideration. Numerical results on the influence of the initial stress, anisotropy properties of the plate material, the crack's length and its distance from the face planes of the plate on the values of the ERR, are presented and discussed. In particular, it is established that for the relatively greater length of the crack's band, the initial stretching of the plate causes a decrease, but the initial compression causes an increase in the values of the ERR.

Keywords: Band crack, energy release rate, stress intensity factor, initial stress, orthotropic material, rectangular plate, 3D FEM.

1 Introduction

It is known that the linear theory of crack mechanics cannot take into consideration the uniformly distributed normal stresses acting along the crack's edges under determination of Stress Intensity Factors (SIF) or Energy Release Rates (ERR) at the tips or fronts of the crack. Note that this state is caused with the linearity of the mathematical modelling as well as with the geometrical modelling of the crack. Nevertheless, up to now within the scope of the T-stress concept [Williams (1957); Rice (1974)] some attempts have been made to take into consideration the aforementioned normal stresses on the crack's growth process

[1] Yildiz Technical University, Department of Mathematical Engineering, Davutpasa Campus, 34220, Esenler, Istanbul-Turkey.

[2] Yildiz Technical University, Faculty of Mechanical Engineering, Department of Mechanical Engineering, Yildiz Campus, 34349, Besiktas, Istanbul-Turkey.

[3] Institute of Mathematics and Mechanics of the National Academy of Science of Azerbaijan, 37041, Baku, Azerbaijan.

within the scope of the linear theory of elasticity. We recall that the T-stress is the first non-singular term in the expansion of the opening normal stress at the near vicinity of the crack's tip or front and this stress has great significance for the prediction of the crack growth direction stability in the fracture of brittle materials [Cotterell and Rice (1980); Melin (2002); Pham, Bahr, Bahr, Fett, and Balke (2006)] and for the determination of the crack growth resistance in the fracture of ductile materials detailed in the paper [Tvergaard and Hutchinson (1994)] and others listed therein. These facts have pushed the researchers to develop mathematical methods for calculation and analysis of the T-stress, some of which are detailed in the papers [Sherry, France, and Goldthorbe (1995); Jogdand and Murthy (2010); Sutradhar and Paulino (2004); Chen (2000); Chen (2014)] and others reviewed therein. Nevertheless, the aforementioned T- stress concept cannot take into consideration the influence of the uniformly distributed normal stresses acting along the crack's edge surfaces on the SIF or ERR. Note that, this influence can be modelled within the framework of the approach of which the equations and relations are obtained from linearization of the corresponding geometrically non-linear field equations and relations of the theory of elasticity. Under this linearization procedure, the stress-strain state regarding the uniformly distributed normal stresses acting along the crack's edge surfaces is taken as the initial stresses, and the non-linear equations and relations are linearized around this initial state and in this way the linearized theory of elasticity is constructed. Consequently, the corresponding crack problems are studied within the scope of this linearized theory, of which the coefficients of the equations and relations contain the aforementioned initial stresses [Guz (1999)]. The fundamentals of the application of the linearized theory on the corresponding crack problems are proposed and detailed in the monograph [Guz (1983)] which also contains many concrete results. A review of more recent results related to the linearized (or so-called, non-classical) crack problems can be found in the papers [Guz (2000); Guz, Dyshel, and Nazarenko (2004)]. However, the results detailed in the works [Guz (1983); Guz (2000); Guz, Dyshel, and Nazarenko (2004)] relate to the micro-crack problems, i.e. to the problems related to the cracks contained in the infinite or semi-infinite elastic medium. Note that up to now some investigations have also been made related to the macro-crack problems [Akbarov and Turan (2009); Akbarov and Turan (2011); Akbarov and Yahnioglu (2016)], the results of which are also detailed in the monograph [Akbarov (2013)]. Moreover, a mixed boundary value problem for an embedded crack in an orthotropic strip is considered in the paper [Yusufoglu and Turhan (2012)]. At the same time, it should be noted that these investigations are carried out for the two-dimensional (plane-strain state) problems and up to now there have not been any investigations regarding the corresponding 3D crack problems. Therefore, in the present paper we attempt to consider and investigate the 3D problem for the band crack contained in the rectangular plate made of anisotropic (orthotropic) material. It is assumed that at first (i.e. in the initial state) the plate's two opposite lateral edge planes are loaded by uniformly distributed normal stretching or compressing forces and then the crack's edge surfaces are loaded with the additional uniformly distributed normal opening forces. It is required to investigate how the uniformly normal initial stresses acting along the crack's edge planes influence the ERR at the band crack front caused with the aforementioned additional opening normal forces acting on the crack's edge planes. Moreover, the influence of the anisotropy properties of the plate material and the crack location with respect to the plate thickness on the ERR is

studied.

2 Formulation of the problem

Consider a rectangular plate and associate the Cartesian coordinate system $Ox_1x_2x_3$ with this plate (Fig. 1). The position of the points of the plate we determine through the Lagrange coordinates in this system. Assume that the plate contains a band crack, the edge plane-surfaces of which are parallel to the plate's face planes. Moreover, we assume that the plate occupies the region

$$\Omega = \{0 \le x_1 \le \ell_1;\ 0 \le x_2 \le h;\ 0 \le x_3 \le \ell_3\} \tag{1}$$

and the crack's upper and lower edge planes occupy the regions Ω_c^+ and Ω_c^-, respectively, where

$$\Omega_c^{\pm} = \{(\ell_1/2 - \ell_0/2) \le x_1 \le (\ell_1/2 + \ell_0/2),\ x_2 = h_c \pm 0,\ 0 \le x_3 \le \ell_3\}. \tag{2}$$

In (1) and (2) the following notation is used: ℓ_1 (ℓ_3) is the plate length in the Ox_1 (Ox_3) axis direction, ℓ_0 is the band crack length in the Ox_1 axis direction, h is the plate thickness, and h_c is the distance of the crack located plane from the lower face plane of the plate (Fig.1).

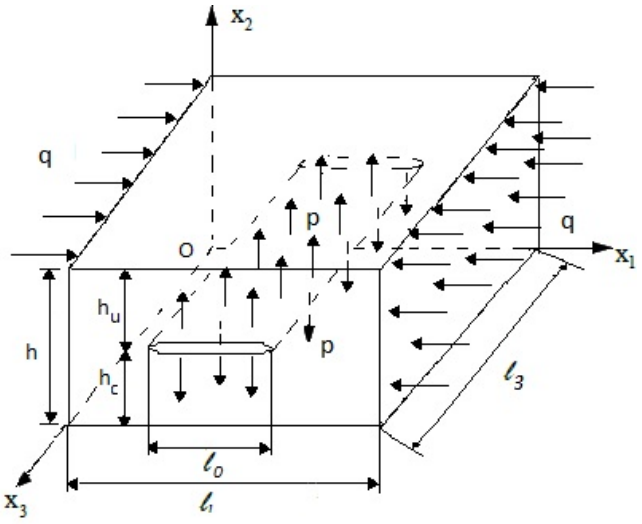

Figure 1: The sketch of the rectangular plate containing the band crack.

We suppose that the material of the plate is orthotropic with the principal axes Ox_1, Ox_2 and Ox_3 of elastic symmetry. Moreover, we suppose that on the plate edge planes at $x_1 = 0$

and $x_1 = \ell_1$ the uniformly distributed normal forces with intensity q act and these forces cause uniformly distributed initial normal stress acting along the crack's edge planes. After this initial stress appears, the crack's edge planes are loaded with additional uniformly distributed normal opening forces with intensity p and assume that $p < q$. Thus, we attempt to investigate how the initial stress influences the ERR caused by the additional opening normal forces with intensity p.

According to the well-known procedure, in the case under consideration the initial stresses caused by the forces with intensity q can be determined as follows

$$\sigma_{11}^0 = q\,,\ \sigma_{ij}^0 = 0 \ \text{for}\ ij \neq 11. \tag{3}$$

In (3) the upper index 0 denotes that the quantities belong to the initial state.

Now we consider formulation of the problem related to the stress-strain state caused by the additional opening normal forces acting on the crack's edge planes. For this purpose we use the so-called three dimensional linearized equations and relations which, for the case under consideration, can be written as follows.

Equilibrium equations and strain-displacement relations.

$$\frac{\partial \sigma_{ji}}{\partial x_j} + \sigma_{11}^0 \frac{\partial^2 u_i}{\partial x_1^2} = 0\,,\ \ \varepsilon_{ij} = \frac{1}{2}\left(\frac{\partial u_i}{\partial x_j} + \frac{\partial u_j}{\partial x_i} \right). \tag{4}$$

In (4) and repeated below, $(i; j = 1,2,3)$ are summed over their ranges and conventional notation is used.

According to [Lekhnitskii (1963)], the constitutive relations for the plate material can be written as follows.

$$\sigma_{11} = A_{11}\varepsilon_{11} + A_{12}\varepsilon_{22} + A_{13}\varepsilon_{33}\,,\ \sigma_{22} = A_{12}\varepsilon_{11} + A_{22}\varepsilon_{22} + A_{23}\varepsilon_{33}\,,$$

$$\sigma_{33} = A_{13}\varepsilon_{11} + A_{23}\varepsilon_{22} + A_{33}\varepsilon_{33}\,,\ \sigma_{23} = 2G_{23}\varepsilon_{23}\,,\ \sigma_{12} = 2G_{12}\varepsilon_{12}\,,\ \sigma_{13} = 2G_{13}\varepsilon_{13}\,. \tag{5}$$

where

$$A_{ij} = \frac{a_{ij}}{\det \left\| a_{ij} \right\|}\,,\ a_{11} = \frac{1}{E_1}\,,\ a_{22} = \frac{1}{E_2}\,,\ a_{33} = \frac{1}{E_3}\,,$$

$$a_{12} = \frac{-\nu_{12}}{E_2}\,,\ a_{13} = \frac{-\nu_{13}}{E_2}\,,\ a_{23} = \frac{-\nu_{23}}{E_3}\,,\ a_{ij} = a_{ji}\,,\ (i; j = 1,2,3). \tag{6}$$

In (5) and (6) the following notation is used: E_1, E_2 and E_3 are the elastic moduli along the principal axes Ox_1, Ox_2 and Ox_3 of the elastic symmetry, respectively; G_{12},

G_{13} and G_{23} are the shear moduli in the Ox_1x_2, Ox_1x_3 and Ox_2x_3 planes, respectively; and ν_{12}, ν_{13} and ν_{23} are Poisson ratios and, according to [Lekhnitskii (1963)], ν_{ij} characterizes the shortening (elongation) in the direction of the $i-th$ axis under tension (compression) along the $j-th$ axis. Moreover, in (6), the symbol "det" means the determinant of the matrix $\|a_{ij}\|$.

Now we consider formulation of the boundary conditions which for the case under consideration are selected as follows.

Boundary conditions on the plate edges at $x_1 = 0, \ell_1$ and $x_3 = 0, \ell_3$:

$$u_2\big|_{x_1=0,\ell_1} = 0\,,\ \left(\sigma_{11} + \sigma_{11}^0 \frac{\partial u_1}{\partial x_1}\right)\Bigg|_{x_1=0,\ell_1} = 0\,,\ \sigma_{13}\big|_{x_1=0,\ell_1} = 0\,,$$

$$u_2\big|_{x_3=0,\ell_3} = 0\,, \sigma_{31}\big|_{x_1=0,\ell_3} = 0\,, \sigma_{33}\big|_{x_1=0,\ell_3} = 0\,. \tag{7$_1$}$$

Boundary conditions on the plate face planes at $x_2 = 0, h$:

$$\sigma_{21}\big|_{x_2=0,h} = \sigma_{22}\big|_{x_2=0,h} = \sigma_{23}\big|_{x_2=0,h} = 0\,. \tag{7$_2$}$$

Boundary conditions on the crack's edge surfaces:

$$\sigma_{22}\big|_{\substack{x_2=h_{c\pm0} \\ (\ell/2-\ell_0/2)<x_1<(\ell/2+\ell_0/2) \\ 0<x_3<\ell_3}} = -p\ ,\ \sigma_{21}\big|_{\substack{x_2=h_{c\pm0} \\ (\ell/2-\ell_0/2)<x_1<(\ell/2+\ell_0/2) \\ 0<x_3<\ell_3}} = 0\,,$$

$$\sigma_{23}\big|_{\substack{x_2=h_{c\pm0} \\ (\ell/2-\ell_0/2)<x_1<(\ell/2+\ell_0/2) \\ 0<x_3<\ell_3}} = 0\ . \tag{7$_3$}$$

Thus, this completes the formulation of the problem, according to which, the determination of the stress-strain state in the rectangular plate containing the band crack is reduced to the solution to the equations (3) – (6) within the scope of the boundary condition given in (7).

3 Method of solution and 3D FEM modelling for calculation of the ERR

As the analytical solution to the problem formulated above is impossible, we attempt to solve it by utilizing the 3D Finite Element Method (FEM). For this purpose, according to [Guz (1999)], we introduce the following functional.

$$\Pi(u_1,u_2,u_3) = \frac{1}{2} \iiint\limits_{\Omega-\Omega_c^- -\Omega_c^+} \Bigg[\left(\sigma_{11} + \sigma_{11}^0 \frac{\partial u_1}{\partial x_1}\right)\frac{\partial u_1}{\partial x_1} + \sigma_{12}\frac{\partial u_1}{\partial x_2} + \sigma_{13}\frac{\partial u_1}{\partial x_3} +$$

$$\left(\sigma_{21}+\sigma_{11}^{0}\frac{\partial u_2}{\partial x_1}\right)\frac{\partial u_2}{\partial x_1}+\ \sigma_{22}\frac{\partial u_2}{\partial x_2}+\left(\sigma_{31}+\sigma_{11}^{0}\frac{\partial u_3}{\partial x_1}\right)\frac{\partial u_3}{\partial x_1}+\sigma_{32}\frac{\partial u_3}{\partial x_2}+\sigma_{23}\frac{\partial u_2}{\partial x_3}+$$

$$\sigma_{33}\frac{\partial u_3}{\partial x_3}\Bigg]dx_1dx_2dx_3-\iint\limits_{\Omega_c^+} p\,u_2\big|_{x_2=h_c+0}dx_1dx_3-\iint\limits_{\Omega_c^-} p\,u_2\big|_{x_2=h_c-0}dx_1dx_3. \tag{8}$$

Employing the usual procedure, we attempt to obtain the equilibrium equations in (4) and the boundary conditions in (7) given for the forces from equating the first variation of the functional Π (8) to zero. The expression of the variation is obtained from (8) as follows.

$$\delta\Pi(u_1,u_2,u_3)=\delta_{u_1}\Pi+\delta_{u_2}\Pi+\delta_{u_3}\Pi=\iiint\limits_{\Omega-\Omega_c^--\Omega_c^+}\Bigg[\left(\sigma_{11}+\sigma_{11}^{0}\frac{\partial u_1}{\partial x_1}\right)\delta\left(\frac{\partial u_1}{\partial x_1}\right)+$$

$$\sigma_{12}\delta\left(\frac{\partial u_1}{\partial x_2}\right)+\sigma_{13}\delta\left(\frac{\partial u_1}{\partial x_3}\right)+\left(\sigma_{21}+\sigma_{11}^{0}\frac{\partial u_2}{\partial x_1}\right)\delta\left(\frac{\partial u_2}{\partial x_1}\right)+\sigma_{22}\delta\left(\frac{\partial u_2}{\partial x_2}\right)+$$

$$\sigma_{23}\delta\left(\frac{\partial u_2}{\partial x_3}\right)+\left(\sigma_{31}+\sigma_{11}^{0}\frac{\partial u_3}{\partial x_1}\right)\delta\left(\frac{\partial u_3}{\partial x_1}\right)+\sigma_{32}\delta\left(\frac{\partial u_3}{\partial x_2}\right)+\ \sigma_{33}\delta\left(\frac{\partial u_3}{\partial x_3}\right)\Bigg]dx_1dx_2dx_3-$$

$$\iint\limits_{\Omega_c^+} p\,\delta u_2\big|_{x_2=h_c+0}dx_1dx_3-\iint\limits_{\Omega_c^-} p\,\delta u_2\big|_{x_2=h_c-0}dx_1dx_3=0. \tag{9}$$

In (9), $\delta\Pi$ is a first variation of the functional Π. $\delta_{u_1}\Pi$, $\delta_{u_2}\Pi$ and $\delta_{u_3}\Pi$ are the variations of the functional Π in Eq. (8) with respect to functions displacements u_1, u_2 and u_3 respectively. The regions Ω, Ω_c^- and Ω_c^+ are determined through the relations (1) and (2).

After some mathematical manipulations, we can represent the equation (9) as follows.

$$\delta\Pi=\iiint\limits_{\Omega-\Omega_c^--\Omega_c^+}\Bigg\{-\left(\frac{\partial}{\partial x_1}\left(\sigma_{11}+\sigma_{11}^{0}\frac{\partial u_1}{\partial x_1}\right)+\frac{\partial}{\partial x_2}\sigma_{21}+\frac{\partial}{\partial x_3}\sigma_{31}\right)\delta u_1-$$

$$\left(\frac{\partial}{\partial x_1}\left(\sigma_{21}+\sigma_{11}^{0}\frac{\partial u_2}{\partial x_1}\right)+\frac{\partial}{\partial x_2}\sigma_{22}+\frac{\partial}{\partial x_3}\sigma_{23}\right)\delta u_2-$$

$$\left(\frac{\partial}{\partial x_1}\left(\sigma_{31}+\sigma_{11}^{0}\frac{\partial u_3}{\partial x_1}\right)+\frac{\partial}{\partial x_2}\sigma_{32}+\frac{\partial}{\partial x_3}\sigma_{33}\right)\delta u_3\Bigg\}dx_1dx_2dx_3-$$

$$\iiint\limits_{\Omega-\Omega_c^- -\Omega_c^+} \left\{ \underline{\frac{\partial}{\partial x_1}\left(\left(\sigma_{11}+\sigma_{11}^0 \frac{\partial u_1}{\partial x_1} \right)\delta u_1 + \left(\sigma_{12}+\sigma_{11}^0 \frac{\partial u_2}{\partial x_1} \right)\delta u_2 + \left(\sigma_{13}+\sigma_{11}^0 \frac{\partial u_3}{\partial x_1} \right)\delta u_3 \right)} - \right.$$

$$\underline{\frac{\partial}{\partial x_2}\left(\sigma_{21}\delta u_1+\sigma_{22}\delta u_2+\sigma_{23}\delta u_3\right)} - \left. \underline{\frac{\partial}{\partial x_2}\left(\sigma_{31}\delta u_1+\sigma_{32}\delta u_2+\sigma_{33}\delta u_3\right)} \right\} dx_1 dx_2 dx_3 -$$

$$\iint\limits_{\Omega_c^+} p\,\delta u_2\big|_{x_2=h_c+0} dx_1 dx_3 - \iint\limits_{\Omega_c^-} p\,\delta u_2\big|_{x_2=h_c-0} dx_1 dx_3 = 0 \ . \qquad (10)$$

Note that the first (the third) underlined term in the equation (10) gives the boundary condition with respect to the forces at $x_1=0$ and $x_1=\ell_1$ (at $x_3=0$ and $x_3=\ell_3$). However, the second underlined term in the equation (10) gives the boundary conditions with respect to the forces given on the lower and upper face planes of the plate (i.e. at $x_2=0$ and $x_2=h$), as well as on the crack's edges, i.e. on Ω_c^+ and Ω_c^-.

Thus, equating the coefficients of δu_1, δu_2 and δu_3 in the equation (10) to zero, the equilibrium equation in (4) and the boundary conditions with respect to the forces in (7) are obtained and in this way, the validity of the functional (8) for the 3D FEM modelling of the boundary value problem under consideration is proven. Note that similar type functional was also used in the paper [Babuscu Yesil (2017)] for investigation of the forced vibration of the pre-stressed rectangular plate with cylindrical cavities.

Now we consider the FEM modelling of the region occupied by the plate. Under this modelling, using the symmetry of the plate geometry and boundary conditions with respect to the planes $x_1=\ell_1/2$ and $x_3=\ell_3/2$, we use a quarter part of the plate which occupies the region

$$\Omega' = \left\{ 0 \le x_1 \le \ell_1/2;\ 0 \le x_2 \le h;\ 0 \le x_3 \le \ell_3/2 \right\}. \qquad (11)$$

According to the FEM procedure, the solution domain Ω' (11) is divided into a finite number of elements, i.e. the domain Ω' is presented as $\Omega' = \bigcup\limits_{k=1}^{M} \Omega'_k$, and Ω'_k is selected as standard rectangular prisms (bricks) with eight nodes. The number M, i.e. the number of finite elements is determined from the convergence requirement of the numerical results.

Note that under the FEM modelling of the crack's front we also use ordinary finite elements, i.e. under this modelling the so-called singular finite elements are not introduced. This is because the investigations carried out in [Akbarov and Turan (2011); Akbarov and Yahnioglu (2016), Akbarov (2013)] show that the use of the singular finite elements under finite element modelling of the crack's tip changes the values of the ERR in an insignificant

amount. Moreover, we note that under FEM modeling the Ω'_k can be also selected as rectangular prisms with nodes the number of which greater than eight. For instance, the Ω'_k can be presented as a 32-node hexahedral element described in [Fan, Zhang, Dong, Li and Atluri (2015)].

Thus, employing the well-known Ritz technique [Zienkiewicz and Taylor (1989)] for the case under consideration we solve numerically the boundary value problem formulated above and in this way we determine the stress-strain state in the plate. After this determination, we calculate the ERR at the crack front with the use of the following algorithm.

First, according to the expression

$$U(S_c)=\frac{1}{2}\iiint\limits_{\Omega-\Omega_c^- -\Omega_c^+} U_0 dx_1 dx_2 dx_3 \tag{12}$$

where

$$U_0=\frac{1}{2}\Bigg[\left(\sigma_{21}+\sigma_{11}^0\frac{\partial u_2}{\partial x_1}\right)\frac{\partial u_2}{\partial x_1}+\left(\sigma_{11}+\sigma_{11}^0\frac{\partial u_1}{\partial x_1}\right)\frac{\partial u_1}{\partial x_1}+\sigma_{12}\frac{\partial u_1}{\partial x_2}+\sigma_{13}\frac{\partial u_1}{\partial x_3}+$$
$$\left(\sigma_{21}+\sigma_{11}^0\frac{\partial u_2}{\partial x_1}\right)\frac{\partial u_2}{\partial x_1}+\sigma_{22}\frac{\partial u_2}{\partial x_2}+$$
$$\left(\sigma_{31}+\sigma_{11}^0\frac{\partial u_3}{\partial x_1}\right)\frac{\partial u_3}{\partial x_1}+\sigma_{32}\frac{\partial u_3}{\partial x_2}+\sigma_{23}\frac{\partial u_2}{\partial x_3}+\sigma_{33}\frac{\partial u_3}{\partial x_3}\Bigg] \tag{13}$$

we calculate the strain energy denoted as $U(S_c)$ where S_c is the area of the crack's edge surface. Thereafter, at a certain point determined with the parameter s/ℓ_1 $(=(0.5\ell_3-x_3)/\ell_1)$ of the crack's front, some perturbation $\Delta S_c(s/\ell_1)$ is added to the area of the crack's edge surface and the strain energy is calculated for this case, i.e. the values of

$$U(S_c+\Delta S_c(s/\ell_1))=\frac{1}{2}\iiint\limits_{\Omega-\Omega_c^- -\Omega_c^+ -\Delta\Omega_c^- -\Delta\Omega_c^+} U_0 dx_1 dx_2 dx_3 \tag{14}$$

are calculated, where $\Delta\Omega_c^-$ and $\Delta\Omega_c^+$ are increments of the domains Ω_c^- and Ω_c^+, respectively caused by the perturbation ΔS_c of the crack's edge area.

Thus, using the expressions in (14) and (12) we determine the values of the ERR (denoted by γ) as follows.

$$\gamma\approx\frac{1}{2}\frac{U(S_c+\Delta S_c(s/\ell_1))-U(S_c)}{\Delta S_c(s/\ell_1)}. \tag{15}$$

Note that under calculation of γ, the magnitude of the area ΔS_c is determined from the convergence of the numerical results obtained for γ with decreasing of ΔS_c.

4 Numerical results and discussions

Below, in consideration of the numerical results, the influence of the initial stress on the ERR will be estimated through the ratio q/E_1, however, the influence of the mechanical constants, i.e. the orthotropic properties of the plate material will be estimated through the ratios G_{12}/E_1, G_{13}/E_1, G_{23}/E_1, E_2/E_1 and E_3/E_1. Moreover, under this consideration we introduce the ratios h/ℓ_1, ℓ_0/ℓ_1, ℓ_3/ℓ_1 and h_u/ℓ_1, where $h_u = h - h_c$. Note that under obtaining these results it is assumed that $\nu_{12} = \nu_{13} = \nu_{23} = 0.3$ and $h/\ell_1 = 0.2$.

All the numerical results which will be discussed below are obtained in the case where the region Ω' (11) is divided into 30, 12 and 30 finite elements in the directions of the Ox_1, Ox_2 and Ox_3 axes, respectively. Moreover, under calculation of the ERR, i.e. under calculation of the values of γ (15), the values of ΔS_c are selected as $\Delta S_c/\ell_1^2 = 5.5\times10^{-4}$. Note that the number of finite elements and the values of ΔS_c are selected from the convergence requirement of the numerical results with accuracy 10^{-5}. Moreover, the PC programs through which the numerical results are obtained, are composed by the authors of the paper and are realized in FTN77.

First, we consider the numerical results illustrating validation of the reliability of the used algorithm and PC programs. For this purpose, we consider the case where the plate material is isotropic, i.e. the case where $E_2/E_1 = E_3/E_1 = 1$, $G_{12}/E_1 = G_{13}/E_1 = G_{23}/E_1 = 1/(2(1+\nu))$ and $\nu = \nu_{12} = \nu_{13} = \nu_{23} = 0.3$. Assume that the initial stress in the plate is absent, i.e. $q/E_1 = 0$ and $h_u = h/2$ under which the crack location and the problem under consideration become symmetric with respect to the $x_2 = h/2$ plane, according to which, we have the crack problem for the mode I. However, in the cases where $h_u \neq h/2$ we have the crack problem for the mixed mode. Consequently, in the case where $h_u = h/2$ we can calculate the SIF, i.e. we can calculate K_I through the values of γ (15) with the use of the well-known expression K_I $(=\sqrt{\gamma/(1-\nu^2)\pi\ell_0})$. According to the well-known mechanical consideration, the results obtained within the

scope of the present algorithm and PC programs for K_I at $s/\ell_1 = 0$ must approach the corresponding ones obtained for the plane strain state with increasing of the ratio ℓ_3/ℓ_1. To prove this prediction, we consider the numerical results given in Tab. 1 which show the values of $K_I / K_{I\infty}$ (where $K_{I\infty} = p\sqrt{\pi\ell_0}$) obtained for various values of the ratios ℓ_0/ℓ_1 and ℓ_0/h. Note that in Tab. 1 the values of $K_I / K_{I\infty}$ related to the plane strain state and denoted as $K_I^S / K_{I\infty}$ are calculated with the use of the analytical expression detailed in the handbook [Sih (1973)]. Thus, analysis of the data illustrated in Tab. 1 proves the foregoing prediction with very high accuracy, i.e. the values of $K_I / K_{I\infty}$ calculated with the use of the present algorithm and PC programs approach $K_I^S / K_{I\infty}$ with increasing of the ratio ℓ_3/ℓ_1. Moreover, according to the mechanical consideration, as $K_{I\infty}$ is the SIF of the mode I in the case where the crack is in the infinite elastic medium, then the ratio $K_I / K_{I\infty}$ must approach 1 with simultaneous decreasing of the ratios ℓ_0/ℓ_1 and ℓ_0/h. Note that this prediction is also proven with the results given in Tab. 1 which are obtained for various ratio ℓ_3/ℓ_1 and in this way the validity of the algorithm and PC programs used in the present investigation are tested and verified.

Table 1: The values of SIF at $s/\ell_1 = 0$ obtained for various values of the ratio ℓ_3/ℓ_1 in the case where the material of the plate is isotropic and the initial stress in the plate is absent.

ℓ_0/ℓ_1	ℓ_0/h	ℓ_3/ℓ_1						
		1	5	10	15	20	50	$K_I^S / K_{I\infty}$ [Sih (1973)]
0.080	0.400	0.9761	1.1771	1.2000	1.2029	1.2036	1.2356	1.2406
0.075	0.375	0.9742	1.1720	1.1922	1.1943	1.1947	1.1948	1.2009
0.060	0.300	0.9278	1.1129	1.1304	1.1329	1.1335	1.1341	1.1444
0.050	0.250	0.8906	1.0658	1.0871	1.0909	1.0920	1.0931	1.0931

Thus, now we consider the numerical results related to the influence of the problem parameters on the values of the dimensionless ERR determined as $\gamma/(p\ell_1^3)$. We also consider the dependence between $\gamma/(p\ell_1^3)$ and s/ℓ_1 ($s = (0.5\ell_3 - x_3)/\ell_1$), i.e. how the crack point distance from the plate's end $x_3 = 0$ influences on $\gamma/(p\ell_1^3)$. For these considerations, we analyze the results given in Tabs. 2, 3 and 4 which illustrate the influence of the ratios ℓ_3/ℓ_1, s/ℓ_1, q/E_1, G_{23}/E_1 (Tab. 2, under $G_{12}/E_1 =$

$G_{13}/E_1=0.1$), G_{12}/E_1 (Tab. 3, under $G_{23}/E_1=G_{13}/E_1=0.1$) and G_{13}/E_1 (Tab. 4, under $G_{12}/E_1=G_{23}/E_1=0.1$) in the case where $E_3/E_1=E_2/E_1=0.5$, $\ell_0/2\ell_1=0.25$ and $h_u/\ell_1=0.1$ (i.e. $h_u=h/2$). It follows from these results that in the relatively small values of the ratio ℓ_3/ℓ_1 (for instance for the case where $\ell_3/\ell_1=1$) the absolute maximum value of the ERR, (as can be predicted) appears at $s/\ell_1=0$ and the values of the ERR monotonically decrease with s/ℓ_1. However, for the relatively greater values of the ratio ℓ_3/ℓ_1 (for instance in the cases where $\ell_3/\ell_1=2$ and 3) in a certain part of the crack front (denoted as $0\le s/\ell_1\le s^*/\ell_1$) the values of the ERR remain approximately constant and under $s/\ell_1>s^*/\ell_1$ the values of the ERR decrease with s/ℓ_1. Note that, according to the data given in Tabs. 2, 3 and 4 it can be taken that $s^*/\ell_1\approx 0.4$ and $s^*/\ell_1\approx 1$ for the cases where $\ell_3/\ell_1=2$ and 3, respectively.

Table 2: The influence of the ratio G_{23}/E_1 on the values of $\gamma/(p\ell_1^3)$ in the various ℓ_3/ℓ_1 , q/E_1 and s/ℓ_1 in the case where $G_{12}/E_1=G_{13}/E_1=0.1$, $E_2/E_1=E_3/E_1=0.5$, $\ell_0/2\ell_1=$ 0.25 and $h_u/\ell_1=0.5h/\ell_1$.

G_{23}/E_1	q/E_1	s/ℓ_1 ($\ell_3/\ell_1=1$)						
		0	0.03	0.1	0.2	0.3	0.36	0.4
0.1	-0.01	22.4196	22.3137	21.4884	18.3288	12.753	7.8909	2.9469
	0	13.7697	13.7254	13.1533	11.8825	8.8454	5.8233	2.3612
	0.01	9.5049	9.4871	9.3305	8.6141	6.8231	4.7522	3.4568
0.05	-0.01	27.6317	27.5539	26.9055	24.3008	16.429	13.333	5.9291
	0	16.9657	16.9472	16.7838	15.9965	12.265	10.391	5.0978
	0.01	11.7580	11.7579	11.7743	11.7016	10.820	8.8186	7.0541
		s/ℓ_1 ($\ell_3/\ell_1=2$)						
		0	0.2	0.4	0.6	0.73	0.8	0.86
0.1	-0.01	28.3165	28.5390	28.7312	26.3608	20.389	15.431	9.4171
	0	15.9994	16.1381	16.4526	15.8959	13.207	10.506	6.8140
	0.01	10.5282	10.5992	10.8283	10.8240	9.5547	7.9512	5.4498
0.05	-0.01	32.772	32.8424	32.7727	30.9957	26.304	21.687	14.939
	0	18.972	18.9856	18.9817	18.6702	17.255	15.232	11.410
	0.01	12.7603	11.7743	11.7016	11.8004	12.580	11.800	9.5144
		s/ℓ_1 ($\ell_3/\ell_1=3$)						
		0	0.6	0.9	1	1.1	1.2	1.3

0.1	-0.01	30.9739	31.4613	31.9778	31.2755	29.091	24.397	16.496
	0	17.3966	17.5582	18.0691	18.0336	17.364	15.341	11.140
	0.01	11.3317	11.3797	11.7095	11.8273	11.688	10.779	8.3722
0.05	-0.01	34.7238	34.9761	35.0308	34.5291	33.101	29.277	22.752
	0	19.7975	19.8684	19.8775	19.8259	19.414	18.758	15.873
	0.01	13.0817	13.1043	12.9833	12.9796	13.100	13.208	12.239

Table 3: The influence of the ratio G_{12}/E_1 on the values of $\gamma/(p\ell_1^3)$ in the various ℓ_3/ℓ_1 , q/E_1 and s/ℓ_1 in the case where $G_{23}/E_1 = G_{13}/E_1 = 0.1$, $E_2/E_1 = E_3/E_1 = 0.5$, $\ell_0/2\ell_1 =$ 0.25 and $h_u/\ell_1 = 0.5h/\ell_1$.

G_{12}/E_1	q/E_1	s/ℓ_1 ($\ell_3/\ell_1=1$)						
		0	0.03	0.1	0.2	0.3	0.36	0.4
0.1	-0.01	22.4196	22.3137	21.4884	18.3288	12.753	7.8909	2.9469
	0	13.7697	13.7254	13.1533	11.8825	8.8454	5.8233	2.3612
	0.01	9.5049	9.4871	9.3305	8.6141	6.8231	4.7522	3.4568
0.05	-0.01	36.9888	36.7496	34.8144	28.3804	18.388	10.464	6.9465
	0	18.3204	18.2374	17.5588	15.1016	10.662	6.7160	4.6076
	0.01	11.4425	11.4120	11.1515	10.0736	7.7003	5.2014	3.7167
		s/ℓ_1 ($\ell_3/\ell_1=2$)						
		0	0.2	0.4	0.6	0.73	0.8	0.86
0.1	-0.01	28.3165	28.5390	28.7312	26.3608	20.389	15.431	9.4171
	0	15.9994	16.1381	16.4526	15.8959	13.207	10.506	6.8140
	0.01	10.5282	10.5992	10.8283	10.8240	9.5547	7.9512	5.4498
0.05	-0.01	59.4964	59.4485	57.6707	48.4793	34.116	24.401	13.986
	0	23.3897	23.6312	23.9270	22.2096	17.443	13.378	8.3248
	0.01	13.0614	13.1854	13.5231	13.6452	11.418	9.2818	6.1848
		s/ℓ_1 ($\ell_3/\ell_1=3$)						
		0	0.6	0.9	1	1.1	1.2	1.3
0.1	-0.01	30.9739	31.4613	31.9778	31.2755	29.091	24.397	16.496
	0	17.3966	17.5582	18.0691	18.0336	17.364	15.341	11.140
	0.01	11.3317	11.3797	11.7095	11.8273	11.688	10.779	8.3722
0.05	-0.01	66.8953	66.9283	66.9283	63.0712	55.659	43.635	27.262
	0	25.9496	26.4227	27.0723	26.6093	24.930	21.151	14.586
	0.01	14.2577	14.3679	14.8824	14.9846	14.643	13.233	9.9246

Table 4: The influence of the ratio G_{13}/E_1 on the values of $\gamma/(p\ell_1^3)$ in the various ℓ_3/ℓ_1 , q/E_1 and s/ℓ_1 in the case where $G_{12}/E_1 = G_{23}/E_1 = 0.1$, $E_2/E_1 = E_3/E_1 = 0.5$, $\ell_0/2\ell_1 =$ 0.25 and $h_u/\ell_1 = 0.5h/\ell_1$.

G_{13}/E_1	q/E_1	s/ℓ_3 ($\ell_3/\ell_1=1$)						
		0	0.03	0.1	0.2	0.3	0.36	0.4
0.1	-0.01	22.4196	22.3137	21.4884	18.3288	12.753	7.8909	2.9469
	0	13.7697	13.7254	13.1533	11.8825	8.8454	5.8233	2.3612
	0.01	9.5049	9.4871	9.3305	8.6141	6.8231	4.7522	3.4568
0.05	-0.01	22.0752	21.9584	21.0068	17.6241	11.784	6.9517	4.5526
	0	13.2181	13.1680	12.7489	11.1250	7.9252	4.9490	3.3565
	0.01	8.9495	8.9282	8.7419	7.9187	5.9964	3.9568	2.7750
		s/ℓ_3 ($\ell_3/\ell_1=2$)						
		0	0.2	0.4	0.6	0.73	0.8	0.86
0.1	-0.01	28.3165	28.5390	28.7312	26.3608	20.389	15.431	9.4171
	0	15.9994	16.1381	16.4526	15.8959	13.207	10.506	6.8140
	0.01	10.5282	10.5992	10.8283	10.8240	9.5547	7.9512	5.4498
0.05	-0.01	27.4571	27.8129	28.3319	26.0447	19.685	14.508	8.4808
	0	15.2527	15.4588	15.9621	15.4782	12.524	9.6561	5.9580
	0.01	9.9055	10.0142	10.3668	10.4273	8.9491	7.1956	4.6759
		s/ℓ_3 ($\ell_3/\ell_1=3$)						
		0	0.6	0.9	1	1.1	1.2	1.3
0.1	-0.01	30.9739	31.4613	31.9778	31.2755	29.091	24.397	16.496
	0	17.3966	17.5582	18.0691	18.0336	17.364	15.341	11.140
	0.01	11.3317	11.3797	11.7095	11.8273	11.688	10.779	8.3722
0.05	-0.01	30.1893	30.8428	31.8617	31.2387	28.921	23.836	15.519
	0	16.7773	16.9874	17.7865	17.8137	17.067	14.767	10.244
	0.01	10.8312	10.8941	11.4134	11.5863	11.400	10.291	7.5781

At the same time, the results given in Tabs. 2, 3 and 4 show that a decrease in the values of the shear modulus G_{23} and G_{12} causes an increase in the values of the ERR and the magnitude of this increase is considerable. However, the influence of a decrease of the shear modulus G_{13} on the ERR is insignificant. Besides all of these, the foregoing results show that the initial stretching (compressing) of the plate in the Ox_1 axis direction (Fig. 1) causes a decrease (an increase) in the values of the ERR. Note that the influence of the initial stress on the values of the ERR depends also on the geometrical parameters such as

ℓ_0 / ℓ_1 (dimensionless crack's length) and h_u / ℓ_1 (the distance of the crack from the upper face plane of the plate). This dependence is illustrated with the results given in Tabs. 5 and 6 which are obtained for various $\ell_0 / 2\ell_1$ (Tab. 5, under $h_u / \ell_1 = 0.5h / \ell_1$) and h_u / ℓ_1 (Tab. 6, under $\ell_0 / 2\ell_1 = 0.25$) in the case where $G_{23} / E_1 = G_{13} / E_1 = G_{12} / E_1 = 0.1$, $E_3 / E_1 = E_2 / E_1 = 0.5$ and $s / \ell_1 = 0$. It follows from Tabs. 5 and 6 that an increase in the crack length ℓ_0 / ℓ_1 and a decrease in the values of the ratio h_u / ℓ_1 cause an increase in the values of the ERR and an increase in the magnitude of the influence of the initial stress q / E_1 on the ERR.

Table 5: The values of $\gamma / (p\ell_1^3)$ calculated at $s / \ell_1 = 0$ and obtained for various $\ell_0 / 2\ell_1$ and q / E_1 in the case where $G_{12} / E_1 = G_{23} / E_1 = G_{13} / E_1 = 0.1$, $E_2 / E_1 = E_3 / E_1 = 0.5$, $\ell_3 / \ell_1 = 1$ and $h_u / \ell_1 = 0.5h / \ell_1$.

$\ell_0 / 2\ell_1$	q / E_1			
	0	$\frac{+0.001}{-0.001}$	$\frac{+0.005}{-0.005}$	$\frac{+0.01}{-0.01}$
0.10	1.5054	$\frac{1.4744}{1.5377}$	$\frac{1.3622}{1.6816}$	$\frac{1.2440}{1.9020}$
0.15	3.7503	$\frac{3.6461}{3.8599}$	$\frac{3.2740}{4.3616}$	$\frac{2.9036}{5.1713}$
0.20	7.6623	$\frac{7.3974}{7.9436}$	$\frac{6.4790}{9.2639}$	$\frac{5.58040}{11.5054}$
0.25	13.7697	$\frac{13.2100}{14.3694}$	$\frac{11.3078}{17.2556}$	$\frac{9.5049}{22.4196}$

Table 6: The values of $\gamma / (p\ell_1^3)$ calculated at $s / \ell_1 = 0$ and obtained for various h_u / ℓ_1 and q / E_1 in the case where $G_{12} / E_1 = G_{23} / E_1 = G_{13} / E_1 = 0.1$, $E_2 / E_1 = E_3 / E_1 = 0.5$, $\ell_3 / \ell_1 = 1$ and $\ell_0 / 2\ell_1 = 0.25$.

h_u / ℓ_1	q / E_1			
	0	$\frac{+0.001}{-0.001}$	$\frac{+0.005}{-0.005}$	$\frac{+0.01}{-0.01}$
0.10	13.7697	$\frac{13.2100}{14.3694}$	$\frac{11.3078}{17.2556}$	$\frac{9.5049}{22.4196}$

0.0833	14.6570	$\frac{14.0107}{15.3549}$	$\frac{11.8495}{18.7900}$	$\frac{9.8517}{25.2556}$
0.0666	17.9324	$\frac{16.9306}{19.0396}$	$\frac{13.7435}{24.8809}$	$\frac{11.0160}{37.7048}$
0.0500	26.1155	$\frac{23.9975}{28.5639}$	$\frac{17.8596}{43.4137}$	$\frac{13.3117}{88.5157}$

Numerical results given in Tab. 7 show that the influence of the change of the ratios E_3 / E_1 and E_2 / E_1 on the ERR is insignificant. Note that these results are obtained in the case where $G_{23} / E_1 = G_{13} / E_1 = G_{12} / E_1 = 0.1$, $\ell_0 / 2\ell_1 = 0.25$, $h_u / \ell_1 = 0.5h / \ell_1$, $\ell_3 / \ell_1 = 1$ and $s / \ell_1 = 0$.

Table 7: The influence of the ratios E_2 / E_1 and E_3 / E_1 on the values of $\gamma / (p\ell_1^3)$ calculated at $s / \ell_1 = 0$ for various q / E_1 in the case where $G_{12} / E_1 = G_{23} / E_1 = G_{13} / E_1 = 0.1$, $\ell_0 / 2\ell_1 = 0.25$, $\ell_3 / \ell_1 = 1$ and $h_u / \ell_1 = 0.5h / \ell_1$.

E_3/E_1	E_2/E_1							
	0.5				0.3			
	q / E_1				q / E_1			
	0	$\frac{+0.001}{-0.001}$	$\frac{+0.005}{-0.005}$	$\frac{+0.01}{-0.01}$	0	$\frac{+0.001}{-0.001}$	$\frac{+0.005}{-0.005}$	$\frac{+0.01}{-0.01}$
0.5	13.7697	$\frac{13.2100}{14.3694}$	$\frac{11.3078}{17.2556}$	$\frac{9.5049}{22.4196}$	14.1682	$\frac{13.5992}{14.7777}$	$\frac{11.6625}{17.7054}$	$\frac{9.8229}{22.9249}$
0.3	12.6710	$\frac{12.2055}{13.1668}$	$\frac{10.6018}{15.5119}$	$\frac{9.0484}{19.5597}$	12.9163	$\frac{12.4567}{13.4050}$	$\frac{10.8668}{15.7046}$	$\frac{9.3165}{19.6325}$

Now we turn again to consideration of the results related to the influence of the initial stress q / E_1 on the ERR. We recall that, according to the results discussed above, the initial stretching (compressing) of the plate causes to decrease (to increase) the ERR. However, under initial compression of the plate at a certain value of the compression force q / E_1, buckling delamination around the crack takes place and this "certain" value is called the critical value and is denoted through q_{cr} / E_1. Note that corresponding buckling delamination problems are investigated in the papers [Akbarov and Yahnioğlu (2010); Akbarov, Yahnioğlu, and Karatas (2010)] and also are detailed in the monograph [Akbarov

(2013)]. Thus, the numerical results obtained in the present investigations show that if the plate is compressed initially and the absolute values of the ratio q/E_1 increase and approach q_{cr}/E_1, then the values of the ERR increase monotonically and approach infinity as $q/E_1 \to q_{cr}/E_1$. For illustration of this statement, the dependence between $\gamma/(p\ell_1^3)$ and q/E_1 is given graphically in Figs. 2 and 3 which are constructed for the case where $\ell_3/\ell_1=1$, $G_{13}/E_1=0.1$, $E_3/E_1=E_2/E_1=0.5$, and $h_u/\ell_1=0.5h/\ell_1$. In these figures, the graphs grouped by the letter a (by the letter b) are constructed at $s/\ell_1=0$ (at $s/\ell_1=0.4$). The graphs given in Fig. 2 (in Fig. 3) are constructed for various values of the ratio G_{23}/E_1 under $G_{12}/E_1=0.1$ (of the ratio G_{12}/E_1 under $G_{23}/E_1=0.1$). Note that in these figures the values of q_{cr}/E_1 are also indicated by the vertical dashed lines. As the influence of the change of G_{23}/E_1 on the values of q_{cr}/E_1 is insignificant and as the values coincide with each other with very high accuracy, therefore in Fig. 2, q_{cr}/E_1 is indicated only for the case where $G_{23}/E_1=0.1$. However, as the influence of the change of G_{12}/E_1 on q_{cr}/E_1 is considerable, therefore, in Fig. 3, all the values of q_{cr}/E_1 which correspond to the selected values of G_{12}/E_1, are indicated.

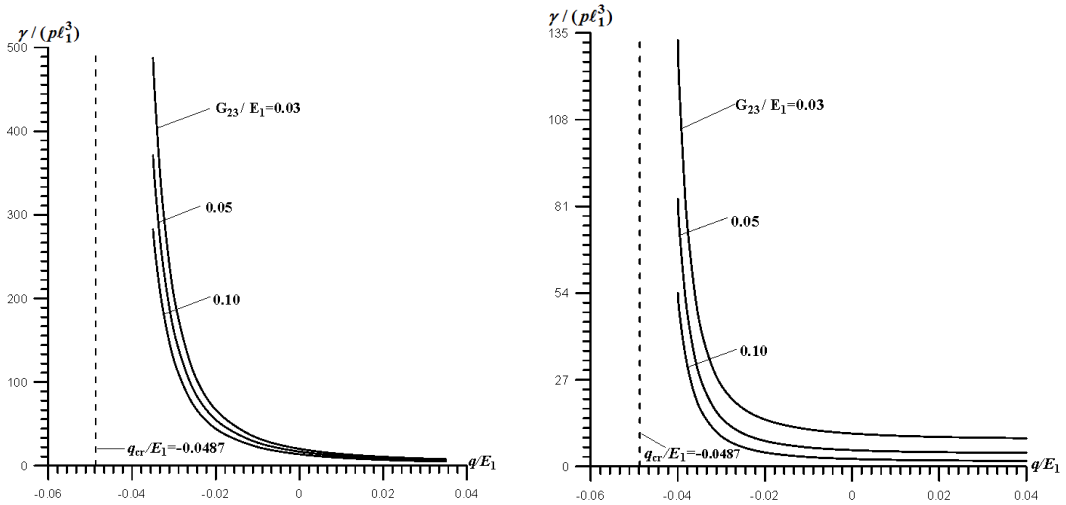

Figure 2: Graphs of the dependence between $\gamma/(p\ell_1^3)$ and q/E_1 constructed for various G_{23}/E_1 in the cases where $s/\ell_1=0$ (a) and $s/\ell_1=0.4$ (b) under $G_{12}/E_1=G_{13}/E_1=0.1$, $E_2/E_1=E_3/E_1=0.5$, $\ell_3/\ell_1=1$ and $\ell_0/2\ell_1=0.25$.

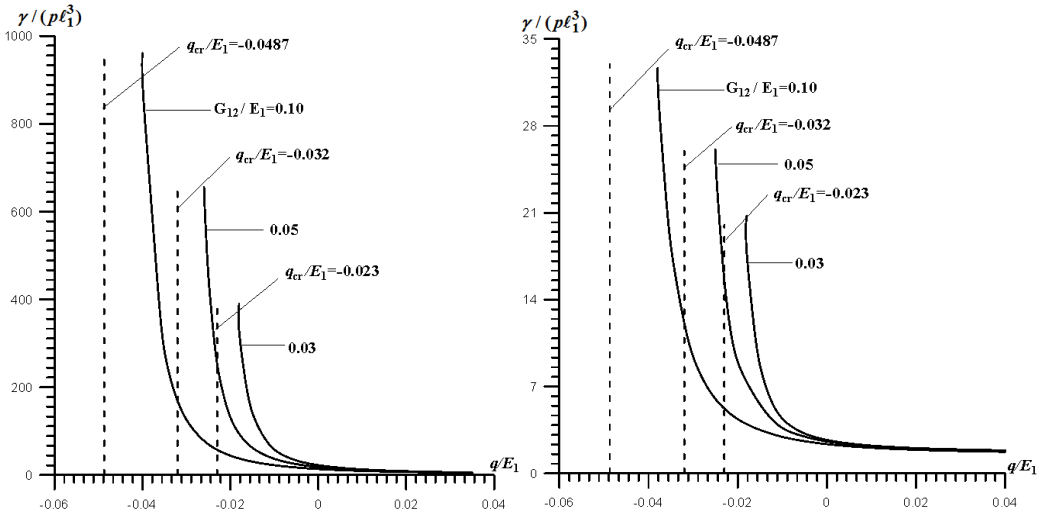

Figure 3: Graphs of the dependence between $\gamma/(p\ell_1^3)$ and q/E_1 constructed for various G_{12}/E_1 in the cases where $s/\ell_1 = 0$ (a) and $s/\ell_1 = 0.4$ (b) under $G_{23}/E_1 = G_{13}/E_1 = 0.1$, $E_2/E_1 = E_3/E_1 = 0.5$, $\ell_3/\ell_1 = 1$ and $\ell_0/2\ell_1 = 0.25$.

We recall that all the numerical results discussed above are obtained in the cases where $\ell_3/\ell_1 \geq 1$ and it is established that the initial stretching of the plate causes a decrease, but the initial compression causes an increase of the ERR. The detailed numerical investigation carried out for the cases where $\ell_3/\ell_1 < 1$ shows that the character of the influence of the initial stress of the plate on the ERR remains valid before a certain value of the ratio ℓ_3/ℓ_1 (denote it as $(\ell_3/\ell_1)^* < 1$) but after this the character changes. In other words, in the cases where $\ell_3/\ell_1 < (\ell_3/\ell_1)^*$ the initial stretching of the plate causes an increase, but the initial compression causes a decrease of the ERR. For a clear illustration of this statement, we consider the graphs of the dependence between $\gamma_d/(p\ell_1^3)$ (where $\gamma_d = (\gamma|_{q/E_1 \neq 0} - \gamma|_{q/E_1=0}) / \gamma|_{q/E_1=0}$)and q/E_1. These graphs are given in Figs. 4 and 5 which are constructed for various ℓ_3/ℓ_1 under $G_{13}/E_1 = 0.1$, $E_3/E_1 = E_2/E_1 = 0.5$, $h_u/\ell_1 = 0.5h/\ell_1$ and $s/\ell_1 = 0$ for the cases where $G_{23}/E_1 = 0.05$ (Fig. 4a) and $G_{23}/E_1 = 0.03$ (Fig. 4b) for $G_{13}/E_1 = 0.1$ and for the cases where $G_{12}/E_1 = 0.05$ (Fig. 5a) and $G_{12}/E_1 = 0.03$ (Fig. 5b) for $G_{23}/E_1 = 0.1$.

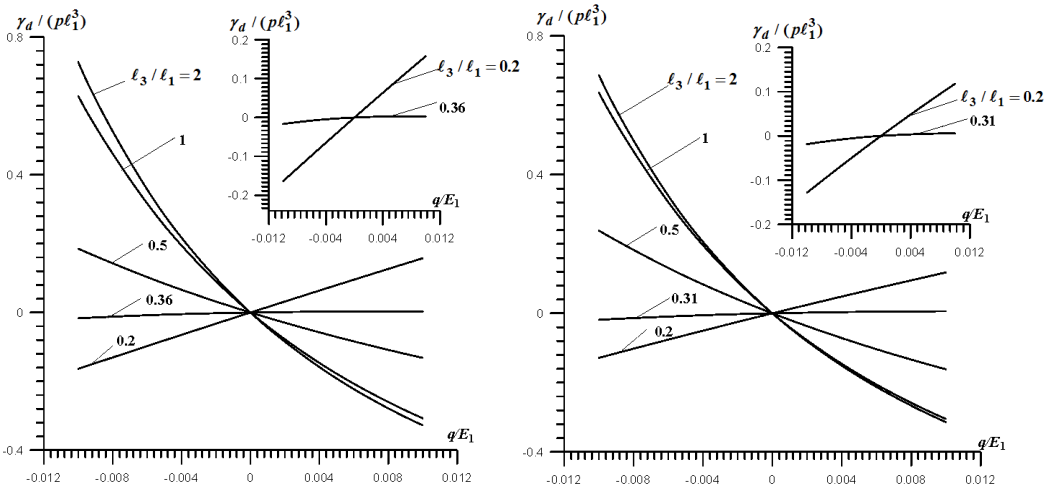

(a) (b)

Figure 4: The graphs of the dependence between $\gamma_d/(p\ell_1^3)$ change γ_d $\left(=\left(\gamma\big|_{q/E_1\neq 0}-\gamma\big|_{q/E_1=0}\right)/\gamma\big|_{q/E_1=0}\right)$ as a result of the initial stress and the ratio ℓ_3/ℓ_1 in the cases where $G_{23}/E_1=0.05$ (a) and $G_{23}/E_1=0.03$ (b) under $G_{12}/E_1=G_{13}/E_1=0.1$, $E_2/E_1=E_3/E_1=0.5$, $\ell_0/2\ell_1=0.25$ and $s/\ell_1=0$

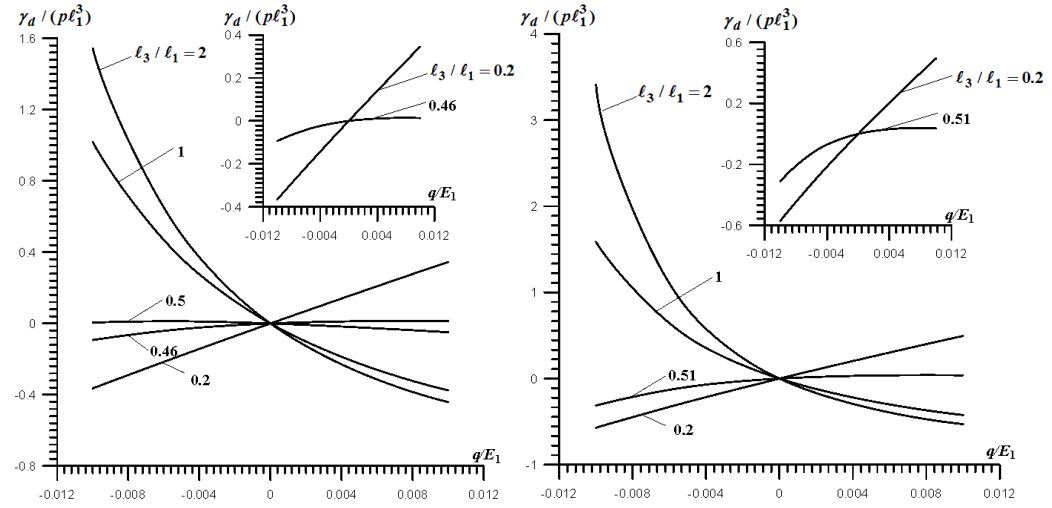

(a) (b)

Figure 5: The graphs of the dependence between the ERR change $\gamma_d/(p\ell_1^3)$ (where

$\gamma_d = (\gamma|_{q/E_1\neq 0} - \gamma|_{q/E_1=0}) / \gamma|_{q/E_1=0})$ as a result of the initial stress and the ratio ℓ_3/ℓ_1 in the cases where $G_{12}/E_1 = 0.05$ (a) and $G_{12}/E_1 = 0.03$ (b) under $G_{23}/E_1 = G_{13}/E_1 = 0.1$, $E_2/E_1 = E_3/E_1 = 0.5$, $\ell_0/2\ell_1 = 0.25$ and $s/\ell_1 = 0$.

Note that the aforementioned change of the character of the influence of the initial stress of the plate on the values of the ERR can be explained with the three-dimensionality of the problem under consideration and with the restriction of the crack's opening displacements, with the condition $u_2 = 0$ on the surfaces of the ends of the plate at $x_3 = 0$, and $x_3 = \ell_3$.

Now we attempt to describe the possible method for experimental determination of the influence of the initial stresses on the ERR. First of we note that for this purpose it is necessary to appear the homogeneous initial stretching or compressing stress in the specimen-plate or specimen-beam acting along the direction which is parallel to the crack's edges and perpendicular to the crack's front. According to this statement, in the present case it is impossible to use the double cantilever beam (DCB) specimens which are used almost all experimental studies of the ERR (see, for instance the paper [Shah and Tarfaoui (2017)] and many others listed therein) at a crack tip in the classical cases. Consequently, in order to appear the aforementioned initial stresses it is necessary to use the specimen which contain the band crack and to apply firstly corresponding external forces for appearing the initial stresses and then to apply the additional external forces for opening the crack' edges. Namely, determining experimentally the values of the displacements caused by these additional forces and using the corresponding plate or beam theory, such as in [Shah and Tarfaoui (2017)], it can be calculated the corresponding ERR experimentally. It should be noted that, in the present case the mentioned plate or beam theories must take into consideration of the corresponding initial stretching or compressing of that.

5 Conclusions

Thus, in the present paper, the mathematical modelling and 3D FEM study of the ERR are undertaken in the band crack's front contained in the orthotropic thick rectangular plate which is stretched or compressed initially before the loading of the crack's edge planes. The initial stretching or compressing of the plate causes the uniformly normal stress acting in the direction which is parallel to the plane on which the band crack is located, to appear. After the appearance of the initial stress in the plate it is assumed that the crack's edge planes are loaded with additional uniformly distributed normal forces and the ERR caused with this additional loading is studied.

The corresponding boundary value problem is formulated within the scope of the so-called 3D linearized theory of elasticity which allows us to take into consideration the initial stress on the values of the ERR but it is impossible to study this influence within the scope of the 3D linear theory of elasticity. Under formulation of the problem related to determination of the stress-strain state which is caused by, among other conditions, the aforementioned additional loading acting on the crack's edge planes on the plate ends, it is also assumed that the displacement along the plate thickness is equal to zero.

The problem under consideration is solved numerically by employing the 3D FEM. Numerical results on the influence of the initial stress, orthotropic properties of the plate material, crack's length and its distance from the upper face plane of the plate on the values of the ERR, are presented and discussed. According to these results and discussions the following concrete conclusions can be drawn.

- Before a certain length of the crack's band, the initial stretching of the plate causes a decrease, but that initial compression causes an increase in the values of the ERR;
- In the cases where the crack's band length is less than the aforementioned "certain length", the character of the influence of the initial stress on the ERR changes and this change may be caused by the restriction of the band's ends opening displacement;
- The magnitude of the influence of the initial stress on the ERR increases with the crack length and with the convergence of the crack to the plate's upper plane;
- A decrease in the values of the shear modulus of the plate material in the planes which are perpendicular to the crack's location plane causes a considerable increase in the values of the ERR;
- Under initial compression of the plate, the values of the ERR approach infinity with the approaching of the absolute values of the initial compression force to the critical force which causes the buckling-delamination of the plate around the band crack;
- Under a relatively greater length of the crack's band, the values of the ERR obtained in a certain part of the crack's front which is around the center of this front along the band direction, can be taken as the corresponding ones related to the plane strain state.

References

Akbarov, S. D.; Turan, A. (2009): Mathematical modelling and the study of the influenc e of initial stresses on the SIF and ERR at the crack tips in a plate-strip of orthotropic mat erial. *Appl. Math. Model*, vol. 33, no. 9, pp. 3682 - 3692.

Akbarov, S. D.; Yahnioglu, N. (2010): Delamination buckling of a rectangular orthotropic c omposite plate containing a band crack. *Mech. Comp. Mater*, vol. 46, no. 5, pp. 493 - 504.

Akbarov, S. D.; Yahnioglu, N.; Karatas, E.E. (2010): Buckling delamination of a recta ngular plate containing a rectangular crack and made from elastic and viscoelastic compo site materials. *Int. J. Solid Structures*, vol. 47, no 25, pp. 3426 - 3434.

Akbarov, S. D.; Turan, A. (2011): On the energy release rate at the crack tips in a finite pre-strained strip. *CMC Comp. Mater. Cont.*, vol.24, no. 3, pp. 257 - 270.

Akbarov, S. D. (2013)**:** *Stability Loss and Buckling Delamination: Three-dimensional Li nearized Approach for Elastic and Viscoelastic Composites*. Springer, Verlag - Berlin.

Akbarov, S. D.; Yahnioglu, N. (2016): On the total electro-mechanical potential energy and energy release rate at the interface crack tips in an initially stressed sandwich plate-str ip with piezoelectric face and elastic core layers. *Int. J. Solids Structures*, vol. 88-89, pp.1 19-130.

Babuscu, Y.U. (2017): Forced and natural vibrations of an orthotropic pre-stressed rectan gular plate with neighboring two cylindrical cavities. *CMC Comp. Mater. Cont.*, vol. 53,

no. 1, pp. 1-23.

Chen, Y.Z. (2000): Closed form solutions of T-stress in plane elasticity crack problems. *Int. J. Solids. Struct*, vol. 37, no. 1, pp. 1763- 1783.

Chen Y. Z. (2014): Evaluation of the T-stress for multiple cracks in an elastic half-plane using singular integral equation and Green's function method. *Appl. Math. Comp*, vol. 22 8, pp. 17-30.

Cotterell, B.; Rice, J. R. (1980): Slightly curved or kinked cracks. *Int. J. Fract*, vol. 16, n o. 2, pp. 155-169.

Fan, Q.; Zhang, Y.; Dong, L.; Li, S.; Atluri, S. N. (2015): Static and dynamic analysis of la minated thick and thin plates and shells by a very simple displacement-based 3-D hexahedral element with over-integration. *CMC Comp. Mater. Cont.*, vol.47, no. 2, pp. 65 - 68.

Guz, A. N. (1983): *Brittle Fracture Mechanics of Prestressed Materials*, Naukova Dumk a, Kiev (in Russian).

Guz, A. N. (1999): *Fundamentals of the Three-dimensional Theory of Stability of Deform able Bodies*, Springer, Verlag-Berlin.

Guz, A. N. (2000): Description and study of some nonclassical problems of fracture mech anics and related mechanisms, *Int. Appl. Mech.*, vol. 36, no.12, pp. 1537-1564.

Guz, A. N.; Dyshel, M. S.; Nazarenko, V. M. (2004): Fracture and stability of materials and structural members with cracks: approaches and results. *Int. Appl. Mech.*, vol. 40, no. 12, pp. 1323-1359.

Jogdand, P. V.; Murthy, K. S. R. K. (2010): A finite element based interior collocation method for the computation of stress intensity factors and T-stresses. *Eng. Fract. Mech.*, v ol. 77, no. 7, pp. 1116-1127.

Lekhnitskii, S. G. (1963): *Theory of Elasticity of an Anisotropic Body*, Holden Day, San Francisco.

Melin, S. (2002): The influence of the T-stress on the directional stability of cracks. *Int. J. Fract.*, vol. 114, no. 3, pp. 259-265.

Pham, V. B.; Bahr, H. A.; Bahr, U.; Fett, T.; Balke, H. (2006): Crack paths and the proble m of global directional stability. *Int. Journal of Fracture*, vol. 141, no. 3-4, pp. 513-534.

Rice, J. R. (1974): Limitations to the small, scale yielding approximation of elastic–plasti c crack-tip fields. *J. Mech. Phys. Solids*, vol. 22, pp.17-26.

Shah, O. R.; Tarfaoui, M. (2017): Determination of mode I & II strain energy release rat es in composite foam core sandwiches. An experimental study of the composite foam cor e interfacial fracture resistance. *Composites Part B*, vol. 111, pp. 134 - 142

Sih, G. (1973): *Handbook of Stress Intensity Factors*, Lehigh University.

Sherry, A. H.; France, C. C.; Goldthorpe, M. R. (1995): Compendium of T-stress solut ions for two and three dimensional cracked geometries. *Fatigue* Fract. *Eng. Mater. Struc t.*, vol. 18, pp. 141–155.

Sutradhar, A.; Paulino, G. H. (2004): Symmetric Galerkin boundary element computati on of T-stress and stress intensity factors for mixed-mode cracks by the interaction integr al method. *Eng. Anal. Boundary Elem.*, vol. 28, no. 11. pp. 1335-1350.

Tvergaard, V.; Hutchinson, J. V. (1994): Effect of T-stress on mode I crack growth resi stance in a ductile solid. *Int. J. Solids. Structures*, vol. 31, no. 6, pp. 823-833.

Williams, M. L. (1957): On the stress distribution at the base of a stationary crack. *ASME J. Appl. Mech.*, vol. 22, pp. 111-114.

Yusufoglu, E.; Turhan, I. (2012): A mixed boundary value problem in orthotropic strip containing a crack, *J. Franklin Inst*, vol. 349, no. 6, pp. 2750-2769.

Zienkiewicz, O. C.; Taylor, R. L. (1989): *The Finite Element Method, Basic Formulatio n and Linear Problems*, 4-th ed., vol.1, McGraw-Hill Book Company, London, 1989.